European Journal of Pharmaceutics and Biopharmaceutics 141 (2019) 139–148

Contents lists available at ScienceDirect

European Journal of Pharmaceutics and Biopharmaceutics

journal homepage: www.elsevier.com/locate/ejpb

Research paper

Preparation and evaluation of celecoxib-loaded proliposomes with high lipid content

Daeun Jeon[a,1], Ki-Taek Kim[a,b,1], Min-Jun Baek[a], Dong Hyun Kim[c], Jae-Young Lee[c,*], Dae-Duk Kim[a,**]

[a] College of Pharmacy and Research Institute of Pharmaceutical Sciences, Seoul National University, Seoul 08826, Republic of Korea
[b] College of Pharmacy and Natural Medicine Research Institute, Mokpo National University, Jeonnam 58554, Republic of Korea
[c] College of Pharmacy, Chungnam National University, Daejeon 34134, Republic of Korea

ARTICLE INFO

Keywords:
Proliposomes
Solid dispersion
High lipid content
Celecoxib
Oral bioavailability
Pharmacokinetic study

ABSTRACT

A novel proliposomal formulation for improved oral delivery of celecoxib (CXB) was developed using a solid dispersion technique. CXB, soy phosphatidylcholine (SPC), sorbitol, and poloxamer 188 were dissolved in a water/ethanol binary solvent system. Subsequent solvent-evaporation and lyophilization steps produced CXB-loaded proliposomes (CXBPLs) with high lipid content (as SPC, ≈20% [*w/w*]). Powder X-ray diffractometry and differential scanning calorimetry analyses revealed that the physical state of CXB was transformed from crystalline to amorphous after the preparation process. Reconstitution of CXBPLs with gentle shaking by hand generated CXB-loaded liposomes with nano-sized mean diameter, negative zeta potential, vesicular-shaped morphology, and high CXB entrapment efficiency (≈84.7%). CXBPLs exhibited improved dissolution rate and permeability compared with free CXB and Celebrex (a commercial product of CXB). In the pharmacokinetic study performed in rats, the CXBPL-treated group showed a 1.7-fold increase in the bioavailability of CXB compared with the free CXB-treated group ($p < 0.05$). The histological observation with hematoxylin and eosin staining demonstrated no additional detrimental effect of CXBPLs on the intestinal epithelia of rats compared with that of free CXB. These results suggest that the developed proliposomes provide an efficient and safe way of enhancing the oral bioavailability of poorly water-soluble drugs.

1. Introduction

Celecoxib (CXB) is a selective cyclooxygenase (COX)-2 inhibitor, which is used to treat osteoarthritis, rheumatoid arthritis, ankylosing spondylitis, primary dysmenorrhea, and acute pain [1]. Although CXB possesses superior pharmacological effects over non-selective COX inhibitors (375-fold improved selectivity) [2], its poor water-solubility (≈5 μg/mL) and slow dissolution rate resulted in the low and variable oral bioavailability, thereby limiting its therapeutic efficacy [3,4]. As CXB belongs to the biopharmaceutical classification system (BCS) class II (low solubility and high permeability), increasing its solubility and dissolution rate may improve the oral bioavailability [5,6]. In the previous studies, several formulation techniques, such as solid dispersion [7], spherical agglomeration [8], nanosuspension [9], nanoparticles [10], and spray-drying [11], were employed to overcome this limited dissolution of CXB, and all of those strategies successfully enhanced systemic exposure of CXB in the *in vivo* pharmacokinetic studies.

Liposomes, together with the above approaches, could also be useful to address the dissolution problem of CXB. Liposomes are spherical vesicles composed of phospholipid bilayers, which are conventionally made by hydration of thin lipid film. By virtue of the characteristic structure, liposomes can accommodate both hydrophobic and hydrophilic drugs within the phospholipid membrane and the internal aqueous compartment, respectively, with high loading capacity [12]. Extensive studies on liposomal drug delivery systems suggest that this formulation can improve the solubility and gastrointestinal (GI) permeability of the loaded drugs, which may result in an enhanced oral bioavailability [12–14]. However, liposomes also have drawbacks, such as complexity of the preparation methods, instability during storage (aggregation, precipitation, fusion, and decomposition of phospholipids), high cost compared with the low product yield, and poor

* Corresponding author.
** Corresponding author.
E-mail addresses: jaeyoung@cnu.ac.kr (J.-Y. Lee), ddkim@snu.ac.kr (D.-D. Kim).
[1] These authors contributed equally to this work.

https://doi.org/10.1016/j.ejpb.2019.05.025
Received 11 September 2018; Received in revised form 20 May 2019; Accepted 28 May 2019
Available online 28 May 2019
0939-6411/

reproducibility of the final products, all of which hamper their use in clinical applications [15–18].

Proliposomes (PLs) are a solid formulation that can rapidly transform into liposomal structures when dispersed in aqueous media [16], of which pharmaceutical characteristics make up for the demerits of liposomes. For example, the preparation methods of PLs are relatively simple and cost-effective than those of liposomes [16]. Given the dry and solid properties, PLs are also more stable than the conventional liposomes during storage [19]. Moreover, the proliposomal powder has free-flowing property [20], so that it can be further modified into various dosage forms including tablets and capsules [19,21]. Along with these advantages, PLs exhibited promising results in enhancing the oral bioavailability of poorly water-soluble drugs [17,22,23].

Conventionally, PLs were prepared by coating water-soluble materials (*e.g.*, carbohydrates or proteins) with phospholipids using a rotary evaporator [24], a coating pan [19], or a fluidized bed [25]. The PLs made by these techniques exhibited low lipid contents and can only generate the micro-sized liposomes (or liposomal agglomerates) without further processes like sonication or high-pressure homogenization, limiting their production in large-scale and application in clinics [24,25]. In this work, PLs with a high lipid content (≈20%, *w/w*) were prepared for effective oral delivery of CXB by applying the solid dispersion technique consisting of only simple mixing, evaporation, and lyophilization steps. The developed PLs were able to produce nano-sized liposomes without the above-mentioned manipulations, suggesting their feasibility for a scaled-up production [26,27]. Physicochemical properties of the CXB-loaded PLs were characterized in both the solid and liposomal states. Meticulous studies on the *in vitro* Caco-2 permeability and *in vivo* pharmacokinetic properties in rats were performed, as well as the *in vitro* dissolution tests.

2. Materials and methods

2.1. Materials

Celecoxib (CXB) and Celebrex were gifted from Hanlim Pharm. Co., Ltd. (Seoul, Korea). Soy phosphatidylcholine (SPC; Lipoid S75, fat-free soybean phospholipids with 70% PC, Lipoid GmbH, Ludwigshafen, Germany) was donated by Phytos (Anyang, Korea). Ethanol and dimethyl sulfoxide (DMSO) were purchased from Daejung Chemicals & Metals Co., Ltd. (Seoul, Korea). Poloxamer 188 was obtained from BASF (Ludwigshafen, Germany). Sorbitol, sodium dodecyl sulfate (SDS), DiI, 4-(2-hydroxyethyl)piperazine-1-ethanesulfonic acid (HEPES), Hank's balanced salt solution (HBSS), sodium bicarbonate, and D-glucose were purchased from Sigma–Aldrich (St. Louis, MO, USA). Dulbecco's modified Eagle medium (DMEM), penicillin, streptomycin, and fetal bovine serum (FBS) were obtained from Gibco Life Technologies, Inc. (Carlsbad, CA, USA). All other reagents were of analytical grade.

2.2. Preparation of CXB-loaded proliposomes (CXBPLs)

CXBPLs were prepared according to the method previously reported by our group with modification (Fig. 1) [28]. Briefly, SPC (800 mg), poloxamer 188 (40 mg), and CXB (100 mg) were dissolved in ethanol (8.75 mL) by vortex-mixing to obtain a clear yellow solution. Sorbitol (3160 mg) was dissolved in double-deionized water (DDW; 3.75 mL). The two solutions were mixed in a round-bottom flask with gentle stirring for 30 min. The mixture was then evaporated under vacuum for 10 min at 40 °C using a rotary evaporator. After the removal of ethanol, the resulting solution was immediately lyophilized. The obtained CXBPLs were ground using a pestle and mortar. The powder that had the size between the US sieve No. 25 and 100 was collected. The pale-yellow powder was stored at −20 °C for further experiments. The blank PLs were prepared with the same method except for the absence of CXB in the ethanol phase.

2.3. Characterization of CXBPLs in solid state

The morphology of CXBPLs was observed by using a field emission-scanning electron microscopy (FE-SEM; JSM-6700F; JEOL, Tokyo, Japan) at an accelerating voltage of 10 kV. Before the observation, the samples were placed on a carbon-taped stub and sputter-coated with platinum under vacuum for 120 s.

To measure the CXB content (%), CXBPLs (10 mg) were dissolved in a co-solvent composed of acetonitrile (ACN) and DDW (50:50, *v/v*) with sonication for 30 min. The solution was diluted with a mobile phase consisting of ACN with 0.1% triethylamine (TEA) and phosphate buffer (10 mM; pH 9.0) with 0.1% TEA (70:30, *v/v*). The CXB concentration of the sample was determined using high-performance liquid chromatography (HPLC) system, equipped with a Waters e1525 separation module and a Waters 2487 dual λ absorbance detector (Waters Co., Milford, MA, USA). The wavelength for the detection was set at 260 nm. The separation was carried out using an isocratic elution at a flow rate of 1.0 mL/min. An aliquot (20 μL) of the sample was injected into a C18 Gemini-NX column (250 × 4.6 mm, 5 μm; Phenomenex, Torrance, CA, USA) with a C18 guard column (4 × 2.0 mm; Phenomenex), and the retention time of CXB was 5.2 min. The standard sample of 200 ng/mL was selected as the lowest concentration of the calibration curve for this quantification method.

Differential scanning calorimetry (DSC) analysis was conducted using a DSC-Q1000 (TA Instrument, New Castle, DE, USA) to evaluate the physical state of CXB in the formulations. CXB, Celebrex, CXBPLs, blank PLs, and the excipients used were weighed and sealed in aluminum pans, and the thermal transition was scanned from 0 to 200 °C at a heating rate of 10 °C/min. An empty pan was used as a reference. Powder X-ray diffractometry (PXRD) was used to assess the degree of crystallinity of CXB and the other excipients before and after the preparation of PLs. The analyses were performed using a D8 ADVANCE with DAVINCI (BRUKER, German) equipped with Cu $K\alpha_1$ radiation (1.5418 Å). An acceleration voltage and tube current were 40 kV and 40 mA, respectively. Samples were scanned over a 2θ range of 3° to 60° with a step angle of 0.02° at a scan speed of 0.5 sec/step. The physical stability of CXBPLs under the storage condition (kept at −20 °C for 3.5 and 5 months) was also evaluated using these DSC and PXRD methods.

Attenuated total reflectance Fourier transform infrared (ATR-FTIR) spectroscopy (JASCO FT/IR 4200; JASCO Company Ltd., Hachioji, Japan) analyses were conducted to evaluate the molecular interactions. The FTIR spectra of CXB, Celebrex, CXBPLs, and the excipients were recorded over a scanning range of 4000–600 cm^{-1} (resolution: 4.0 cm^{-1}).

2.4. Characterization of liposomes generated by CXBPLs

A liposomal dispersion was generated by reconstituting the PLs (10 mg) in DDW (1 mL) with shaking for 5 min by hand. For the transmission electron microscopy (TEM) observation, a drop of the dispersion was placed onto the surface of a 200-mesh carbon-coated copper grid (Electron Microscopy Sciences, Hatfield, PA, USA) and negatively stained with uranyl acetate. Excess liquid was removed with a filter paper and dried at room temperature. The sample was observed using JEM 1010 (JEOL, Tokyo, Japan) at an accelerating voltage of 80 kV. The mean particle size, polydispersity index (PDI), and zeta potential of the reconstituted liposomes were determined by electrophoretic light-scattering method (ELS-Z; Otsuka Electronics, Tokyo, Japan).

To determine the entrapment efficiency (EE), the liposomal dispersion was filtered through a syringe filter (pore size: 0.45 μm; Minisart RC15; Sartorius, Goettingen, Germany) after the reconstitution process. An aliquot (100 μL) of the filtrate was diluted with ACN (900 μL) to disrupt the liposomal structure. The concentration of CXB in the sample was determined by the HPLC method in Section 2.3.

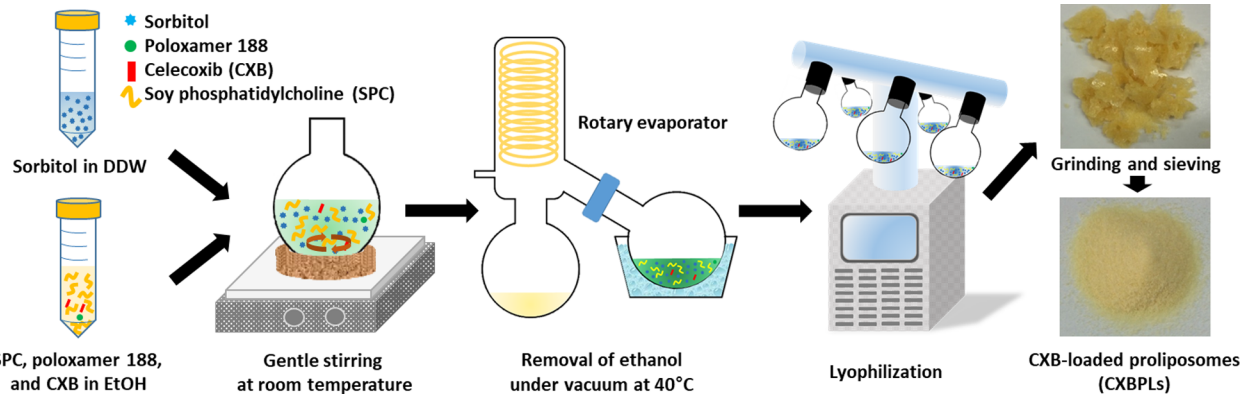

Fig. 1. Schematic illustration of the preparation method of CXBPLs.

2.5. In vitro dissolution studies

Dissolution studies of free CXB, Celebrex, and CXBPLs were performed under sink conditions, where the compositions of dissolution media were determined based on the solubility of CXB in those media. To measure the solubility, CXB (3 mg) was dispersed in the buffered solution (1.5 mL) at various pH values (pH 1.2, 4.0, 6.8 and 12.0) with different SDS concentrations (0, 0.1, 0.4, 0.7, and 1.0% [*w/v*]) in a sample tube by vortex-mixing for 30 min. The tubes were incubated in a shaking water bath (50 rpm) for 48 h at 37 °C, followed by centrifugation at 16,000*g* for 15 min. An aliquot (1 mL) of the supernatant was filtered through a syringe filter (pore size: 0.45 μm; Minisart RC15; Sartorius), and the filtrate was diluted before the analysis by using the HPLC method in Section 2.3.

The dissolution studies were conducted using USP type II dissolution apparatus (TDT-08L; Electrolab, Mumbai, India) with paddle rotating at a speed of 50 rpm. The studies were conducted under various pH conditions (pH 1.2, 4.0, 6.8, and 12.0) at 37.0 ± 0.2 °C. The dissolution media (500 mL) contained SDS (0.4%, *w/v*) to maintain sink conditions. Each formulation equivalent to 2 mg of CXB was encapsulated into a hard gelatin capsule. The capsule was then immersed into the dissolution media with a sinker. Aliquots (1 mL) of the media were collected from the vessels at predetermined time points (15, 30, 45, 60, 90, and 120 min), and an equal volume of fresh medium was replenished after each sampling. The collected samples were immediately filtered through a 0.45 μm syringe filter (Minisart RC15; Sartorius). The filtrate was diluted and analyzed by the HPLC method in Section 2.3.

2.6. Caco-2 permeability test

The Caco-2 cell monolayer model was used to evaluate the *in vitro* permeability of the developed formulations. Caco-2 cells were purchased from Korean Cell Line Bank (Seoul, Korea) and cultured with DMEM supplemented with 10% FBS, 100 U/mL penicillin, and 100 μg/mL streptomycin in a 5% CO_2 atmosphere and 95% relative humidity at 37 °C. The cells were harvested at approximately 90% confluency using 0.5% trypsin-EDTA (Gibco Laboratories, Grand Island, NY, USA) and seeded onto the collagen-coated polytetrafluoroethylene (PTFE) membrane (growth area of 1.12 cm^2 and pore size of 0.4 μm) of the 12-well insert (Transwell®; Corning Inc., Corning, NY, USA) at 2.5 × 10^5 cells/insert. The cell monolayer was used for the experiment after reaching the trans-epithelial electrical resistance (TEER) values over 500 Ω cm^2, which were measured using a Millicell® ERS-2 (Millipore Corporation, Billerica, MA, USA). The TEER values were measured again immediately after the experiment was finished to assess the damage to the cell monolayers during the test.

Absorptive (apical-to-basolateral [A-to-B]) transport studies were carried out in the transport medium (TM) consisting of HBSS, HEPES, sodium bicarbonate, and D-glucose in DDW (pH 7.4). After 30 min of pre-incubation with TM at 37 °C, CXB, Celebrex, or CXBPLs dispersed in TM (500 μL) at a CXB concentration of 500 μM was added to the apical side (A-side) of the insert. The insert was placed into a well filled with fresh TM (1500 μL; B-side) and incubated at 37 °C with continuous agitation (50 rpm). To maintain sink conditions, the insert was moved into another well with fresh TM every 30 min. After 2 h of the total incubation period, each B-side sample was collected, and its CXB concentration was analyzed using HPLC-tandem mass spectrometry (HPLC-MS/MS) system. Each sample (50 μL) was vortex-mixed with ACN (450 μL) containing valsartan (VST; 100 ng/mL as an internal standard [IS]) and loaded into a sample vial. Chromatographic separation was achieved using an Agilent Technologies 1260 Infinity HPLC system (Agilent Technologies, Inc., Palo Alto, CA, USA) equipped with an Agilent Poroshell 120 EC-C18 column (50 × 4.6 mm, 2.7 μm; Agilent Technologies) with a C18 guard column (4 mm × 2.0 mm; Phenomenex), a G1312B binary pump, a G1367E autosampler, a G1316C thermostatted column compartment, and a G1330B thermostat. The isocratic mobile phase consisting of ACN and 5 mM ammonium formate buffer (95:5, *v/v*) was run at a flow rate of 0.4 mL/min. The injection volume was 5 μL, and the total run time was 3 min. Mass spectrometric detection was performed on an Agilent Technologies 6430 Triple Quad LC/MS system with negative electrospray ionization (ESI) mode. The optimized mass transitions from precursor to product ion, fragmentor voltage, and collision energy values were *m/z* 380.2 → 316.2, 170 V, and 19 eV for CXB and *m/z* 434.1 → 350.0, 140 V, and 18 eV for VST, respectively. The data acquisition and processing were performed using MassHunter Workstation Software Quantitative Analysis (Version B.05.00; Agilent Technologies, Inc.). The retention times of CXB and VST were 1.8 and 1.5 min, respectively. The limit of detection (LOD) and lower limit of quantitation (LLOQ) values were determined as 0.5 and 5 ng/mL, respectively, based on the signal-to-noise (S/N) ratio method in the ICH guideline [29]. The apparent permeability value (P_{app}) of each formulation was calculated using the following equation:

$$P_{app} = \frac{\delta Q}{\delta t} \cdot \frac{1}{A \cdot C_0} \ (\text{cm/sec}),$$

where $\delta Q/\delta t$ is the amount of CXB transported across the cell monolayer per unit time, A is the surface area of the monolayer (1.12 cm^2), and C_0 is the initial CXB concentration of the A-side.

2.7. In vivo pharmacokinetic studies

Male Sprague-Dawley (SD) rats with body weights of 235 ± 5 g were obtained from Orient Bio (Sungnam, Korea). The rats were housed in a light-controlled room (12 h of light [07:00–19:00] and 12 h of dark [19:00–07:00] cycles) at a temperature of 22 ± 2 °C and a relative humidity of 55 ± 5% (Animal Center for Pharmaceutical Research,

Table 1
Composition of the developed proliposomal formulations.

Component	Blank PLs	CXBPLs
SPC	20.0% (800 mg)	19.5% (800 mg)
Sorbitol	79.0% (3160 mg)	77.1% (3160 mg)
Poloxamer 188	1.0% (40 mg)	1.0% (40 mg)
CXB	–	2.4% (100 mg)

College of Pharmacy, Seoul National University, Seoul, Korea). Protocols for the animal studies were approved by the Animal Care and Use Committee of the College of Pharmacy, Seoul National University. The femoral artery was cannulated with Intramedic™ polyethylene tubing (PE-50; Becton Dickinson Diagnostics, Sparks Glencoe, MD, USA) under anesthesia with Zoletil® 50 (Virbac, Carros, France) at a dose of 50 mg/kg *via* intramuscular injection. CXB, Celebrex, or CXBPLs was encapsulated into a hard gelatin capsule (size 9; Torpac Inc., Fairfield, NJ, USA) and administered orally at a CXB dose of 2 mg/kg. Blood samples (≈150 μL) were collected from the femoral artery at 1, 5, 15, 30, 45, 60, 90, 120, 240, 360, 480 and 1440 min after the administration, and the same volume of 0.9% sodium chloride injectable solution containing heparin (20 IU/mL) was replenished at each time point. After centrifugation at 16,000*g* for 2.5 min at 4 °C, aliquots (50 μL) of the supernatants (plasma samples) were collected and stored at −20 °C. For the preparation of analytical samples, the plasma samples (50 μL) were vortex-mixed with ACN (200 μL) containing VST (100 ng/mL; IS) for 5 min and centrifuged at 16,000*g* for 5 min. Each supernatant was transferred to a sample vial and analyzed using the HPLC-MS/MS method in section 2.6. Pharmacokinetic parameters were calculated using non-compartmental analysis (WinNonlin, version 3.1, NCA 201; Pharsight, Mountain View, CA, USA): total area under the plasma concentration-time curve from time zero to infinity (AUC), peak plasma concentration (C_{max}), and time to reach C_{max} (T_{max}).

2.8. Histological assay

Histological observations were conducted to evaluate the toxicity of CXB, Celebrex, and CXBPLs to the rat intestinal epithelium. Each formulation was orally administered to SD rats at a CXB dose of 2 mg/kg, and the jejunum was dissected 24 h after the administration. After 24 h of fixation with 4% (*v/v*) formaldehyde solution, the tissue samples were rinsed with DDW, dehydrated with alcohol, and embedded into paraffin. The paraffin blocks were sliced (5 to 10 μm thick), and the sectioned samples were stained with hematoxylin and eosin (H&E) reagent. Microscopic images were acquired using an OLYMPUS IX70 (Tokyo, Japan) microscope.

2.9. Statistical analysis

All the experiments were repeated at least three times, and the data were expressed as the mean ± standard deviation (SD). The statistical analyses (Student's *t*-test and one-way analysis of variance with Bonferroni's multiple comparison test) were performed using the SPSS statistics software (Version 21.0; IBM Corp, NY, USA).

3. Results and discussion

3.1. Preparation and characterization of CXBPLs

Both the solvent evaporation and lyophilization methods were used for the preparation of CXBPLs whereby ethanol and DDW in the intermediate mixture were removed stepwise (Fig. 1). Without the primary solvent evaporation process, the ethanol in the mixture melted down during the lyophilization step (triple point of ethanol: 150 K and 4.3×10^{-4} Pa), extracting out the lipid from the lyophilisate, which compromised the homogeneity of the product (Figure S1a). To overcome this issue, ethanol was evaporated first using the rotary evaporator, and the remaining DDW was removed by subsequent lyophilization. The evaporation temperature was optimized to 40 °C; higher evaporation temperatures increased the mean diameters of liposomes generated from the products (*e.g.*, 1.4-fold increase at 60 °C), and lower temperatures required much longer evaporation time (data not shown).

For the enhancement of the CXB EE and reduction in the total weight of the formulation, a high ratio of lipid to sugar is desired. However, the SPC content over 20% resulted in a product with unfavorable properties including stickiness and low flowability after pulverization (Figure S1b). Thus, the lipid content was set at 20%. In addition, the poloxamer 188 was supplemented to improve the stability of the liposomes after reconstitution [30]. The weight ratio of SPC/sorbitol/poloxamer 188 (blank PLs) in the final formulation was set at 20/79/1 (Table 1). CXBPLs were prepared by adding CXB to the blank proliposomal composition, where the added amount of CXB was optimized by the mean diameter and EE values of the liposomes after reconstitution. As shown in Figure S2a, only the PLs with the CXB amount of 110 mg or below maintained their liposomal mean diameter after reconstitution. In addition, the PLs with the CXB amount of 100 mg or below prevented rapid CXB precipitation, where their EE values were above 80% even 30 min after reconstitution (Figure S2b). Therefore, the CXB amount of 100 mg was finally selected for the preparation of CXBPLs (Table 1).

SEM images of sorbitol, CXB, Celebrex, and CXBPLs are shown in Fig. 2. CXB has more than four types of crystalline polymorphs, and the form III has the most stable structure among them [5]. In our observation, not only CXB but also Celebrex exhibited rod-shaped morphology with the characteristic pinstriped patterns on the particle surface, implying the presence of the crystalline structure [3]. Sorbitol possessed a characteristic acicular-textured surface. Of note, these

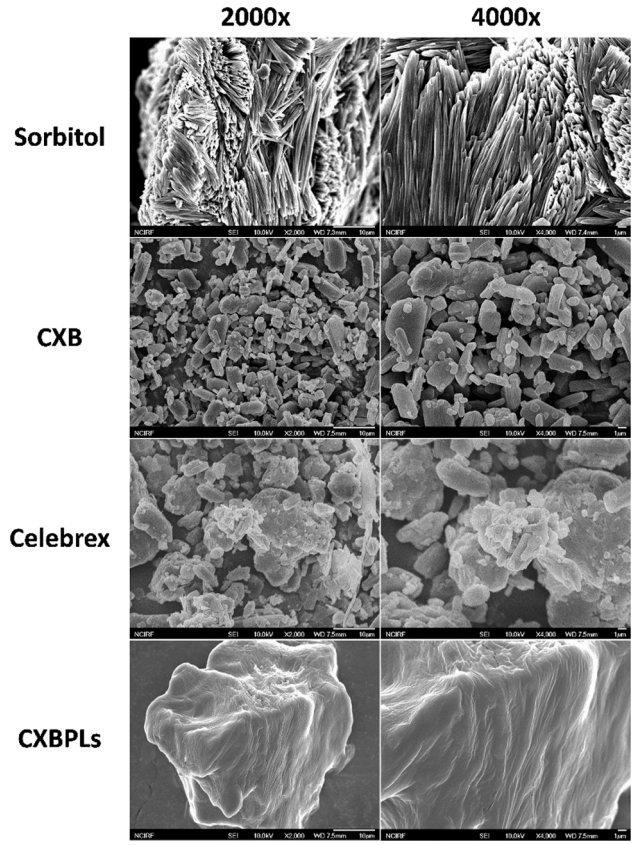

Fig. 2. SEM images of sorbitol, CXB, Celebrex, and CXBPLs. The lengths of the scale bars are 10 μm (left panel) and 1 μm (right panel).

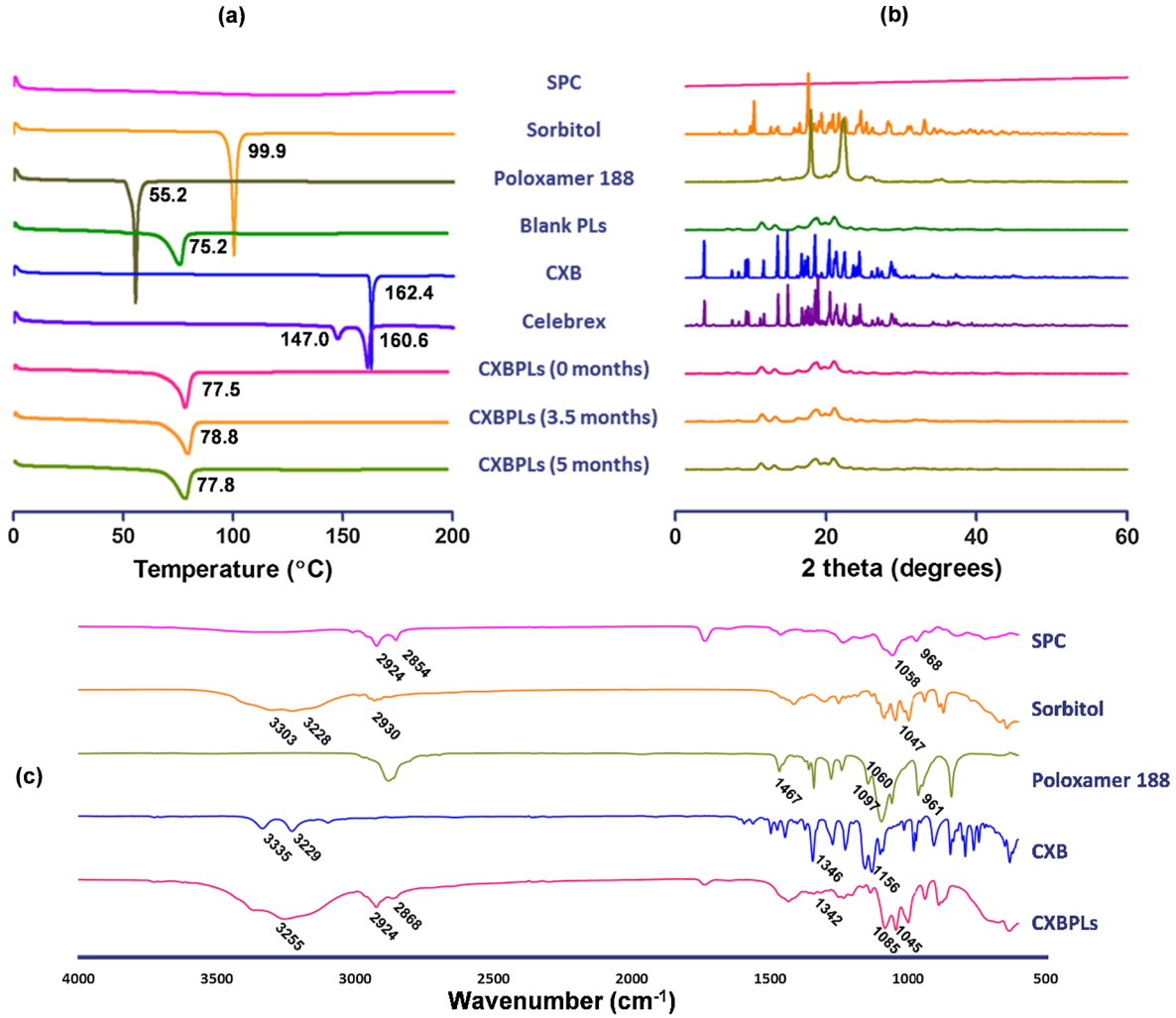

Fig. 3. Characterization of CXBPLs by (a) DSC, (b) PXRD, and (c) FTIR analyses.

distinctive morphologies of CXB and sorbitol completely disappeared in the CXBPL granules, which implies that amorphization occurred during the preparation processes.

More detailed investigations on the crystallinity of CXB were performed using the DSC and PXRD analyses. The DSC curves of CXB, Celebrex, CXBPLs, blank PLs, and the excipients used were presented in Fig. 3a. In general, a crystalline compound exhibits a sharp endothermic peak in the DSC thermogram at its melting temperature, whereas an amorphous one shows no (or gradual) depression [31,32]. Both CXB and Celebrex exhibited sharp endothermic peaks at around 160 °C, which correspond to the melting temperature of CXB crystal (form III) [33]. Sorbitol (γ anhydrous form) and poloxamer 188 also showed endothermic peaks at their melting temperatures [34,35]. However, all of these characteristic sharp peaks disappeared in the thermograms of blank PLs and CXBPLs, indicating the loss of crystallinity during the preparation processes. Instead, a single broad endothermic depression was observed at around 75–79 °C, which could be originated from the residual solvent (*i.e.*, ethanol; boiling point: 78.4 °C). According to the *USP 38 General Chapter ⟨467⟩ Residual Solvents*, ethanol is a *Class 3* solvent (*i.e.*, no human health hazard at pharmaceutical levels), suggesting this issue could hardly be of any toxicity concerns.

The X-ray diffractograms of CXB, Celebrex, CXBPLs, blank PLs, and the excipients were shown in Fig. 3b. As expected from the DSC data, the CXB and Celebrex exhibited the characteristic diffraction peaks of CXB form III (2θ values of 5.4°, 10.7°, 13.0°, 14.8°, 16.1°, 19.6°, and 21.5°), which is in good accordance with the previous report [3]. However, the CXBPLs exhibited a series of broad peaks, of which patterns are almost identical to those of blank PLs. This absence of the distinctive peaks of CXB in the diffractogram of CXBPLs indicates that amorphization of CXB occurred during the preparation of CXBPLs, supporting the above DSC data [31,36]. As shown in Figure S3, the diffractogram of CXBPLs is comparable to that of the physical mixture of crystalline CXB and blank PLs (as CXB, 0.025% [*w/w*]), indicating approximately 99% of the drug molecules in CXBPLs were in the amorphous state. Moreover, the signals of sorbitol and poloxamer 188 were attenuated in the diffractograms of PLs, which could be understood in a similar context.

The amorphous form of CXB can provide increased solubility and dissolution rate compared with its crystalline form because of weaker intermolecular forces [37]. However, due to this metastable property, the amorphous structure can also be converted into the crystals during storage [38]. As the re-crystallization occurs between glass transition temperature and melting temperature, the storage condition at −20 °C was adopted in this study. As evidenced by the DSC and XRD analyses, no signals of evolving crystals were observed even after five months of storage, indicating that CXBPLs was physically stable during this period (Fig. 3a and b).

The FTIR analysis with ATR method was performed to investigate the intermolecular interactions among the components consisting of CXBPLs. The FTIR spectra of CXB, SPC, sorbitol, poloxamer 188, and CXBPLs are shown in Fig. 3c. CXB exhibited symmetric and asymmetric

Table 2
Characterization of the developed proliposomal formulations.

Formulation	Mean diameter (nm)	Polydispersity index	Zeta potential (mV)	Entrapment efficiency (%)[a]	Drug content (%)[b]
Blank PLs	365.6 ± 14.5	0.30 ± 0.02	−59.00 ± 0.09	–	–
CXBPLs	537.1 ± 10.2	0.36 ± 0.01	−64.15 ± 0.26	84.7 ± 1.2	2.35 ± 0.09

Data are presented as the mean ± SD ($n = 3$).
[a] $\text{Entrapmentefficiency}(\%) = \frac{\text{CXBamountinliposomaldispersionafterfiltration(poresize : 0.45}\mu\text{m)}}{\text{totalCXBamountinliposomaldispersionbeforefiltration}} \times 100.$
[b] $\text{Drugcontent}(\%) = \frac{\text{CXBamountinproliosomes}}{\text{totalamountofproliposomes}} \times 100.$

sulfoxide (S═O) stretching bands at 1156 and 1346 cm^{-1}, respectively [6]. The N-H stretching bands at 3335 and 3229 cm^{-1} were also observed [39]. The SPC spectrum showed peaks at 2924 cm^{-1} (aliphatic C—H stretching), 2854 cm^{-1} (olefinic C—H stretching), 1058 cm^{-1} (C—O stretching), and 968 cm^{-1} (C—C stretching). Sorbitol exhibited a broad peak spanning from 3000 to 3500 cm^{-1} (O-H stretching), along with other peaks at 2930 cm^{-1} (aliphatic C—H stretching) and 1047 cm^{-1} (C—O stretching) [40]. Poloxamer 188 also showed its absorption bands at 1467 cm^{-1} (H—C—H in-plane scissoring), 1097 cm^{-1} (C—O—C asymmetric stretching), 1060 cm^{-1} (C—O stretching), and 961 cm^{-1} (C—C stretching) [41,42]. In the CXBPL spectrum, however, the characteristic peaks of the above compounds were shifted, which could be attributed to the intermolecular interactions that occurred during the preparation of PLs.

3.2. Characterization of liposomes generated by CXBPLs

Reconstitution of blank PLs and CXBPLs with gentle shaking by hand generated nano-sized liposomal dispersions with mean diameters of around 370 and 540 nm, respectively (Table 2). The characteristic vesicular structures were confirmed by TEM and confocal laser scanning microscopy (CLSM), indicating the successful conversion from PLs to liposomes (Figures 4 and S4). The morphology of the vesicles exhibited a spherical shape, which is in good accordance with the previous report on the sorbitol-based PLs [43]. The PDI values of blank and CXB-loaded liposomes were revealed to be 0.30 ± 0.02 and 0.36 ± 0.01, respectively (Table 2), suggesting the presence of micron-sized liposomes. However, as can be seen in Figure S4, the sizes of those vesicles were not more than a few microns. This result is in good agreement with the size distribution data acquired by the dynamic light scattering method (Fig. 4). Moreover, it is known that the PDI value of 0.3 is the criterion of particle size homogeneity of liposomal formulations [44]. Both of the PLs showed negative zeta potential values of around −60 mV, which guarantees the high physical stability of the liposomes after reconstitution [45]. The EE of the CXB-loaded liposomes exhibited relatively high values of 84.7 ± 1.2% (Table 2). Noteworthy is that the EE values can vary according to the pore size of the filter used (70.9 ± 4.2% for 0.20 μm and 92.0 ± 4.8% for 5.0 μm), which can be explained by the polydisperse nature of the liposomes. However, the *effective* EE values (*i.e.*, determined with the 0.45 μm filters) are important for understanding the bioavailability of CXBPLs, as the liposomes that are able to pass through this pore size may exhibit the maximum absorption efficiency [46].

3.3. In vitro dissolution studies

The *in vitro* dissolution profiles of free CXB, Celebrex, and CXBPLs are shown in Fig. 5. The dissolution tests were performed at various pH values of 1.2 (enzyme-free simulated gastric fluid), 4.0, 6.8 (enzyme-free simulated intestinal fluid), and 12.0. The sink condition was maintained by adding 0.4% of SDS in the dissolution media, where the CXB solubility values were at least 40-times of the highest theoretical concentration that could be achieved in the dissolution test (Table S1). As shown in Fig. 5, the dissolved CXB amount of free CXB group was no more than 26% at the physiologically relevant pH values (*i.e.*, pH 1.2, 4.0, and 6.8), although its dissolution was markedly increased at pH 12.0 because of the weak acidity ($pK_a \approx 11.1$) [6]. This result is in good agreement with the previous report [37], where the crystalline CXB showed a slow dissolution rate. Celebrex exhibited an improved its dissolution rate than free CXB at pH 4.0 and above, notwithstanding its crystallinity found in the DSC and PXRD analyses (see Section 3.1). This phenomenon may have resulted from SDS (solubilizing agent) and croscarmellose sodium (disintegrant) contained in the Celebrex capsule. At pH 1.2, however, there was no significant difference in dissolution rate between free CXB and Celebrex, which can be explained by the poor swelling property of croscarmellose sodium at this pH value [47]. Interestingly, the dissolved CXB amount from CXBPLs was more than 50% in 30 min even at pH 1.2, and 100% in 120 min at every tested pH value. When compared with the other groups, the dissolved CXB amount of CXBPL group in 120 min was significantly higher ($p < 0.05$) at the physiologically relevant pH conditions (pH 1.2, 4.0, and 6.8). This enhancement in apparent dissolution may be because the reconstitution process of CXBPLs can take place rapidly even with low shear stress, such as gentle shaking by hand. Thus, the CXB in CXBPLs can also be dispersed quickly in the form of CXB-loaded liposomes under the dissolution condition. In addition, the amorphous state of CXB in CXBPLs, as evidenced by the DSC and PXRD studies (see Section 3.1), may have increased its apparent solubility and dissolution rate [39,48]. However, it should be noted that the portion of CXB dissolved at the molecular level (*i.e.*, true solution) was negligible even after the complete dissolution: approximately 0.1% and 2.4% for pH 1.2 and 6.8, respectively, at 120 min (Figure S5). These results suggest that most CXB molecules were in the liposomal membrane after the reconstitution of CXBPLs in the dissolution media. Nonetheless, as CXB is in BCS class II (*i.e.*, high-permeability and low-solubility), the enhancement in apparent dissolution may lead to the improvement in oral bioavailability of CXB as shown in previous reports [5,6,9,49].

3.4. Caco-2 permeability test

Free CXB, Celebrex, and CXBPLs were evaluated for their absorptive transport behavior in the *in vitro* Caco-2 cell monolayer model (Fig. 6), where each formulation was administered to the A-side at a CXB concentration of 500 μM. The average P_{app} value of free CXB was calculated to be 22.8 ± 1.9 nm/sec, which was similar to the result of a previous report (P_{app} = 15.4 ± 10.9 nm/sec) [50]. Of note, significant increases in permeability were observed in Celebrex (P_{app} = 33.2 ± 3.6 nm/sec) and CXBPLs (P_{app} = 101.1 ± 8.0 nm/sec) compared with free CXB ($p < 0.05$). Considering the enhancement in their dissolution properties (see Section 3.3), these results may be due in part to the increased amounts of dissolved CXB in the A-side. Similarly, the significant difference in P_{app} values between Celebrex and CXBPLs ($p < 0.05$) could be explained by the difference in their dissolution properties, as well as the enhancing effects of SPC and poloxamer 188 [51,52].

The TEER measurement was performed before and after the transport experiment to evaluate the damage to the Caco-2 cell monolayer. The average TEER value changes (%) of free CXB-, Celebrex-, and CXBPL-treated monolayers were 78.4 ± 10.9%, 70.3 ± 16.2%, and

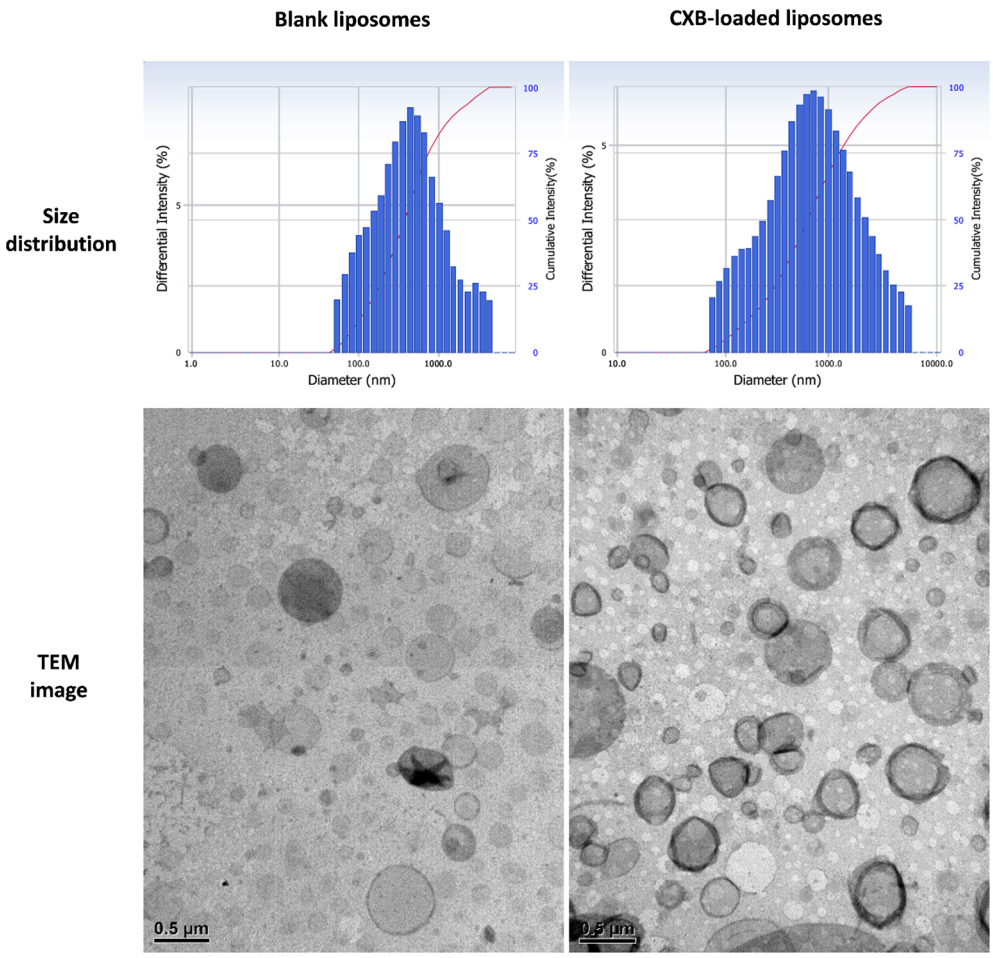

Fig. 4. Size distribution and TEM images of the liposomes generated by the reconstitution of blank PLs and CXBPLs. The length of the scale bar is 500 nm.

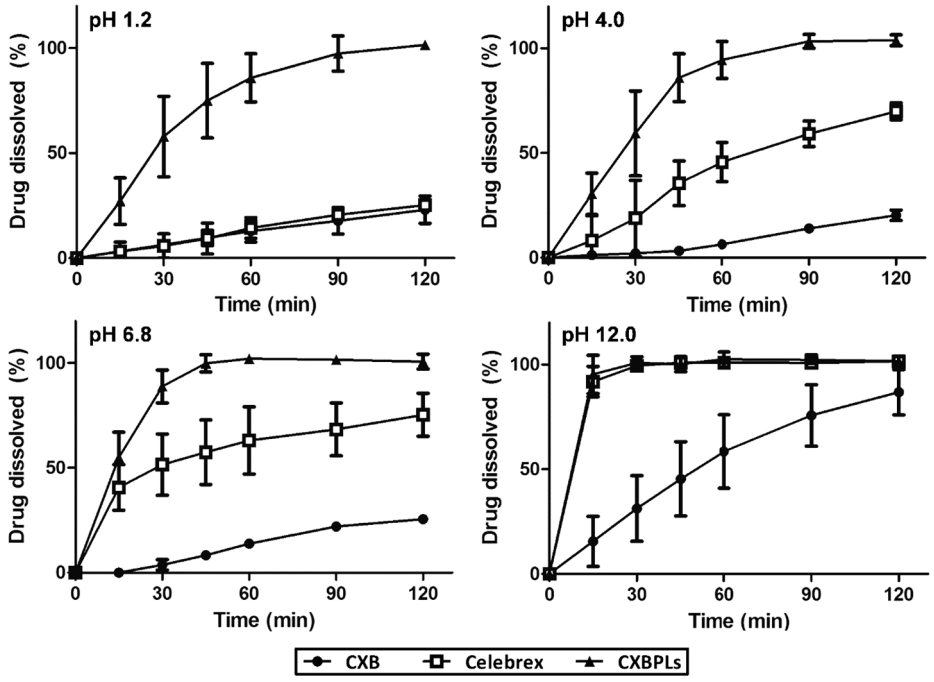

Fig. 5. In vitro dissolution profiles of free CXB, Celebrex, and CXBPLs at pH 1.2, 4.0, 6.8, and 12.0. Data are presented as the mean ± SD (n = 3).

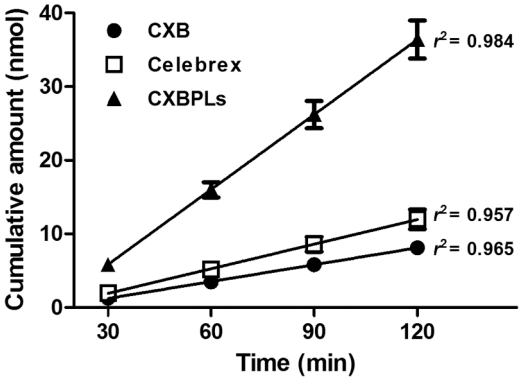

Fig. 6. Cumulative transported amount of CXB across the Caco-2 cell monolayer vs. time after the administration of free CXB, Celebrex, or CXBPLs. A simple linear regression method was used to calculate the P_{app} value of each formulation. Data are presented as the mean ± SD (n = 4).

70.1 ± 3.9%, respectively, showing no significant difference among all groups ($p > 0.05$). Therefore, the permeability enhancement observed in this experiment was not because of the detrimental effect of the formulations on the cell monolayer.

3.5. In vivo pharmacokinetic studies

The *in vivo* pharmacokinetic property of the CXB formulations was evaluated in SD rats. Each formulation (free CXB, Celebrex, or CXBPLs) was administered orally to rats at a CXB dose of 2 mg/kg. The plasma CXB concentration versus time profiles were plotted in Fig. 7, and the corresponding pharmacokinetic parameters (AUC, C_{max}, and T_{max}) were listed in Table 3. The systemic exposure of CXB in the CXBPL-treated group significantly increased by 1.73-fold (as AUC; $p < 0.05$) compared with that of the free CXB-treated group. As the dissolution is the rate-limiting step for the oral absorption of CXB [5,6,37], the improvement in the apparent dissolution rate by the formation of CXB-loaded liposomal dispersion could be the main reason for this enhancement in oral bioavailability (see Section 3.3). Also, this phenomenon can be partly attributed to other mechanisms previously proposed, such as the mixed-micelle formation with endogenous bile acids and the transformation into mesophases [53,54]. The Celebrex-treated group also exhibited a significant increase in AUC (1.67-fold; $p < 0.05$) compared with the free CXB-treated group, which may also have resulted from the improvement in apparent dissolution properties. Comparing the Celebrex- and CXBPL-treated groups, no significant differences in AUC and C_{max} values were observed ($p > 0.05$).

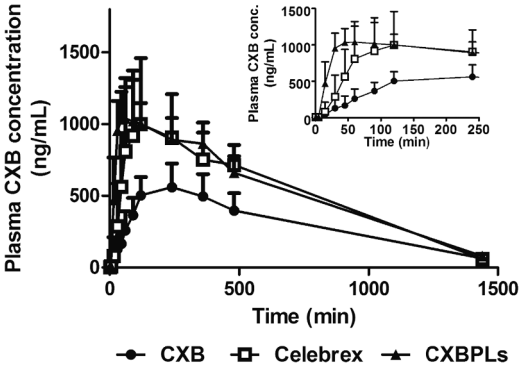

Fig. 7. Plasma concentration vs. time profiles of CXB after a single oral administration of free CXB, Celebrex, and CXBPLs at a dose of 2 mg/kg (inset: an expanded view from time 0 to 250 min). Data are presented as the mean ± SD ($n \geq 3$).

Table 3
Pharmacokinetic parameters after oral administration of free CXB, Celebrex, and CXBPLs at a CXB dose of 2 mg/kg in rats.

Parameter	Free CXB	Celebrex	CXBPLs
AUC (μg min/mL)	464 ± 117	774 ± 165*	803 ± 139*
C_{max} (μg/mL)	0.56 ± 0.17	1.05 ± 0.44	1.12 ± 0.23*
T_{max} (min)	240	165 ± 90	64 ± 19*,+
Relative bioavailability (%)	100	167	173

Data are presented as the mean ± SD (n ≥ 3).
* $p < 0.05$, compared with free CXB group.
\+ $p < 0.05$, compared with Celebrex group.

However, the T_{max} values of the CXBPL-treated group were significantly shorter than those of the other groups ($p < 0.05$). Noteworthy is that the rank order of the average T_{max} values of the formulations (CXBPLs < Celebrex < free CXB, from the shortest to the longest) is closely related to those of the dissolution rate and P_{app} values (see Sections 3.3 and 3.4). As the absorption of CXB took place throughout the GI tract [4], more rapid dissolution and higher permeability of CXB may have caused its faster absorption. A similar approach with CXB-loaded proniosomes consisting of cholesterol, span 60, and dicetyl phosphate was reported by Nasr [49], where the retarded dissolution of CXB from the niosomes delayed its oral absorption with 1.6-fold longer T_{max} than that of Celebrex. For the management of acute pain, however, CXBPLs with shorter T_{max} would be more desirable, providing rapid onset of analgesic effect [55].

3.6. Histological assay

The toxicity of the CXB formulations (free CXB, Celebrex, and CXBPLs) to the intestinal epithelia of rats was evaluated based on the histological assessment by H&E staining (Fig. 8). Although the degree of acute intestinal toxicity caused by the high doses of CXB (50–60 mg/kg) is controversial [37,56], in our investigation with the low dose of CXB (2 mg/kg), no evidence of pathological sign was found in all groups. Moreover, the excipients comprising the CXBPLs (*i.e.*, SPC, sorbitol, and poloxamer 188) are approved by the U.S. FDA for their Generally Recognized as Safe (GRAS) status. SPC is regarded as a non-toxic and non-irritating material. According to a previous report [57], this lipid even reduced the GI toxicity of a COX inhibitor, indomethacin, without lowering the therapeutic efficacy of the drug. Sorbitol, which is a commonly used food additive, also exhibited negligible intestinal

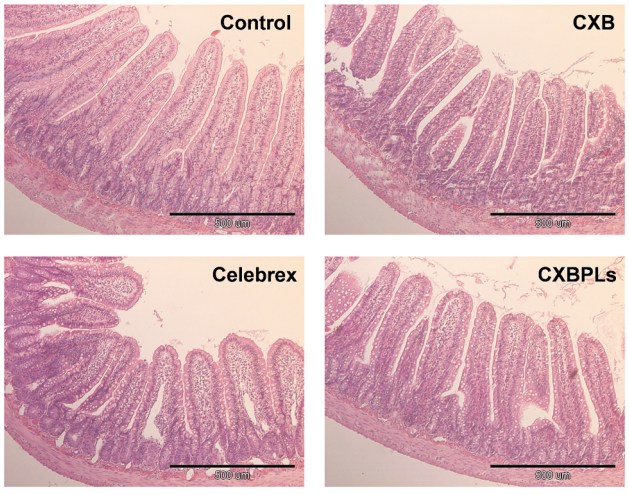

Fig. 8. Morphology of rat intestinal epithelium 24 h after an oral administration of free CXB, Celebrex, or CXBPLs at a dose of 2 mg/kg (H&E staining). The length of the scale bar is 500 μm.

toxicity at its high dose (675–3000 mg/kg) [58]. Thus, the dose administered in our study (around 65 mg/kg) is highly unlikely to be associated with meaningful toxicity in the GI tract. With around 0.85 mg/kg of poloxamer 188, no significant toxicity could be induced, based on the previous report that the exposure to this material up to 5% in the diet caused no adverse effect [59]. Overall, these results suggest that CXBPLs can be used as a biocompatible vehicle for the oral delivery of CXB.

4. Conclusions

A novel proliposomal formulation for the oral delivery of CXB was prepared using solvent-evaporation/lyophilization methods. In the solid-state evaluation with DSC and PXRD analyses, the amorphous state of CXB was observed, which resulted in the increased dissolution rate and apparent permeability of CXBPLs compared with those of free CXB and Celebrex. Pharmacokinetic studies in rats revealed the enhanced oral bioavailability and shorter T_{max} of CXBPLs than those of free CXB and Celebrex. The histological observation confirmed no harmful effect of CXBPLs on the intestinal epithelia of rats in all groups. Taken together, the developed proliposomal system could be a biocompatible platform for enhancing the oral bioavailability of drugs with poor water solubility like CXB.

Acknowledgments

This work was supported by the National Research Foundation of Korea (NRF) grants funded by the Ministry of Science and ICT (Nos. NRF-2018R1A5A2024425 and NRF-2018R1C1B6005379).

Appendix A. Supplementary material

Supplementary data to this article can be found online at https://doi.org/10.1016/j.ejpb.2019.05.025.

References

[1] J. Dong, D. Jiang, Z. Wang, G. Wu, L. Miao, L. Huang, Intra-articular delivery of liposomal celecoxib–hyaluronate combination for the treatment of osteoarthritis in rabbit model, Int. J. Pharm. 441 (2013) 285–290.
[2] D. Clemett, K.L. Goa, Celecoxib: a review of its use in osteoarthritis, rheumatoid arthritis and acute pain, Drugs 59 (2000) 957–980.
[3] S.R. Modi, A.K.R. Dantuluri, V. Puri, Y.B. Pawar, P. Nandekar, A.T. Sangamwar, S.R. Perumalla, C.C. Sun, A.K. Bansal, Impact of crystal habit on biopharmaceutical performance of celecoxib, Cryst. Growth Des. 13 (2013) 2824–2832.
[4] S.K. Paulson, M.B. Vaughn, S.M. Jessen, Y. Lawal, C.J. Gresk, B. Yan, T.J. Maziasz, C.S. Cook, A. Karim, Pharmacokinetics of celecoxib after oral administration in dogs and humans: effect of food and site of absorption, J. Pharmacol. Exp. Ther. 297 (2001) 638–645.
[5] A. Bohr, J. Kristensen, E. Stride, M. Dyas, M. Edirisinghe, Preparation of microspheres containing low solubility drug compound by electrohydrodynamic spraying, Int. J. Pharm. 412 (2011) 59–67.
[6] G. Chawla, P. Gupta, R. Thilagavathi, A.K. Chakraborti, A.K. Bansal, Characterization of solid-state forms of celecoxib, Eur. J. Pharm. Sci. 20 (2003) 305–317.
[7] G.P. Andrews, O. Abu-Diak, F. Kusmanto, P. Hornsby, Z. Hui, D.S. Jones, Physicochemical characterization and drug-release properties of celecoxib hot-melt extruded glass solutions, J. Pharm. Pharmacol. 62 (2010) 1580–1590.
[8] V.R. Gupta, S. Mutalik, M.M. Patel, G.K. Jani, Spherical crystals of celecoxib to improve solubility, dissolution rate and micromeritic properties, Acta Pharm. 57 (2007) 173–184.
[9] A. Dolenc, J. Kristl, S. Baumgartner, O. Planinšek, Advantages of celecoxib nanosuspension formulation and transformation into tablets, Int. J. Pharm. 376 (2009) 204–212.
[10] Y. Liu, C. Sun, Y. Hao, T. Jiang, L. Zheng, S. Wang, Mechanism of dissolution enhancement and bioavailability of poorly water soluble celecoxib by preparing stable amorphous nanoparticles, J. Pharm. Pharm. Sci. 13 (2010) 589–606.
[11] J. Lee, M. Kim, H. Yoon, C. Shim, H. Ko, S. Cho, D. Lee, G. Khang, Enhanced dissolution rate of celecoxib using PVP and/or HPMC-based solid dispersions prepared by spray drying method, J. Pharm. Investig. 43 (2013) 205–213.
[12] S.-S. Hong, S.H. Kim, S.-J. Lim, Effects of triglycerides on the hydrophobic drug loading capacity of saturated phosphatidylcholine-based liposomes, Int. J. Pharm. 483 (2015) 142–150.
[13] X. Zhang, J. Qi, Y. Lu, W. He, X. Li, W. Wu, Biotinylated liposomes as potential carriers for the oral delivery of insulin, Nanomed. Nanotechnol. 10 (2014) 167–176.
[14] C.H. Kim, S.G. Lee, M.J. Kang, S. Lee, Y.W. Choi, Surface modification of lipid-based nanocarriers for cancer cell-specific drug targeting, J. Pharm. Investig. 47 (2017) 203–227.
[15] A. Laouini, C. Charcosset, H. Fessi, R.G. Holdich, G.T. Vladisavljevic, Preparation of liposomes: a novel application of microengineered membranes–from laboratory scale to large scale, Colloids Surf. B Biointerfaces 112 (2013) 272–278.
[16] J. Shaji, V. Bhatia, Proliposomes: a brief overview of novel delivery system, Int. J. Pharm. Bio Sci. 4 (2013) 150–160.
[17] X. Yan-yu, S. Yun-mei, C. Zhi-peng, P. Qi-neng, Preparation of silymarin proliposome: a new way to increase oral bioavailability of silymarin in beagle dogs, Int. J. Pharm. 319 (2006) 162–168.
[18] G.-H. Son, B.-J. Lee, C.-W. Cho, Mechanisms of drug release from advanced drug formulations such as polymeric-based drug-delivery systems and lipid nanoparticles, J. Pharm. Investig. 47 (2017) 287–296.
[19] C. Tantisripreecha, M. Jaturanpinyo, B. Panyarachun, N. Sarisuta, Development of delayed-release proliposomes tablets for oral protein drug delivery, Drug Dev. Ind. Pharm. 38 (2012) 718–727.
[20] K.Y. Janga, R. Jukanti, A. Velpula, S. Sunkavalli, S. Bandari, P. Kandadi, P.R. Veerareddy, Bioavailability enhancement of zaleplon via proliposomes: role of surface charge, Eur. J. Pharm. Biopharm. 80 (2012) 347–357.
[21] M.-Y. Ning, Y.-Z. Guo, H.-Z. Pan, H.-M. Yu, Z.-W. Gu, Preparation and evaluation of proliposomes containing clotrimazole, Chem. Pharm. Bull. 53 (2005) 620–624.
[22] B. Zheng, L. Teng, G. Xing, Y. Bi, S. Yang, F. Hao, G. Yan, X. Wang, R.J. Lee, L. Teng, J. Xie, Proliposomes containing a bile salt for oral delivery of Ginkgo biloba extract: formulation optimization, characterization, oral bioavailability and tissue distribution in rats, Eur. J. Pharm. Sci. 77 (2015) 254–264.
[23] S. Yanamandra, N. Venkatesan, V.G. Kadajji, Z. Wang, M. Issar, G.V. Betageri, Proliposomes as a drug delivery system to decrease the hepatic first-pass metabolism: case study using a model drug, Eur. J. Pharm. Sci. 64 (2014) 26–36.
[24] A.M.A. Elhissi, K.M.G. Taylor, Delivery of liposomes generated from proliposomes using air-jet, ultrasonic, and vibrating-mesh nebulisers, J. Drug Deliv. Sci. Technol. 15 (2005) 261–265.
[25] R.P. Gala, I. Khan, A.M.A. Elhissi, M.A. Alhnan, A comprehensive production method of self-cryoprotected nano-liposome powders, Int. J. Pharm. 486 (2015) 153–158.
[26] C. Chu, S.S. Tong, Y. Xu, L. Wang, M. Fu, Y.R. Ge, J.N. Yu, X.M. Xu, Proliposomes for oral delivery of dehydrosilymarin: preparation and evaluation in vitro and in vivo, Acta Pharmacol. Sin. 32 (2011) 973–980.
[27] Q. Fu, H.L. Fu, L. Huan, W. Zhang, G. Shu, M.J. Liu, F.Y. Deng, J. Hu, Preparation of cefquinome sulfate proliposome and its pharmacokinetics in rabbit, Iran, J. Pharm. Res. 12 (2013) 611–621.
[28] A. Jahn, C.K. Song, P. Balakrishnan, S.S. Hong, J.H. Lee, S.J. Chung, D.D. Kim, AAPE proliposomes for topical atopic dermatitis treatment, J. Microencapsul. 31 (2014) 768–773.
[29] ICH Harmonised Tripartite Guideline, Validation of Analytical Procedures: Text and Methodology Q2(R1), 2005 < https://www.ich.org/fileadmin/Public_Web_Site/ICH_Products/Guidelines/Quality/Q2_R1/Step4/Q2_R1_Guideline.pdf > (accessed 2 February 2019).
[30] G. Wu, J. Majewski, C. Ege, K. Kjaer, M.J. Weygand, K.Y.C. Lee, Interaction between lipid monolayers and poloxamer 188: an X-ray reflectivity and diffraction study, Biophys. J. 89 (2005) 3159–3173.
[31] J. Salonen, L. Laitinen, A.M. Kaukonen, J. Tuura, M. Björkqvist, T. Heikkilä, K. Vähä-Heikkilä, J. Hirvonen, V.P. Lehto, Mesoporous silicon microparticles for oral drug delivery: loading and release of five model drugs, J. Control. Release 108 (2005) 362–374.
[32] H. Yu, Q.-Z. Zhai, Mesoporous SBA-15 molecular sieve as a carrier for controlled release of nimodipine, Microporous Mesoporous Mater. 123 (2009) 298–305.
[33] R.B. Chavan, S.R. Modi, A.K. Bansal, Role of solid carriers in pharmaceutical performance of solid supersaturable SEDDS of celecoxib, Int. J. Pharm. 495 (2015) 374–384.
[34] M. Mathlouthi, G. Benmessaoud, B. Rogé, Role of water in the polymorphic transitions of small carbohydrates, Food Chem. 132 (2012) 1630–1637.
[35] A. Homayouni, F. Sadeghi, A. Nokhodchi, J. Varshosaz, H.A. Garekani, Preparation and characterization of celecoxib solid dispersions; comparison of poloxamer-188 and PVP-K30 as carriers, Iran, J. Basic Med. Sci. 17 (2014) 322–331.
[36] S. Kapoor, R. Hegde, A.J. Bhattacharyya, Influence of surface chemistry of mesoporous alumina with wide pore distribution on controlled drug release, J. Control. Release 140 (2009) 34–39.
[37] P. Zhao, H. Jiang, T. Jiang, Z. Zhi, C. Wu, C. Sun, J. Zhang, S. Wang, Inclusion of celecoxib into fibrous ordered mesoporous carbon for enhanced oral bioavailability and reduced gastric irritancy, Eur. J. Pharm. Sci. 45 (2012) 639–647.
[38] S.K. Sathigari, V.K. Radhakrishnan, V.A. Davis, D.L. Parsons, R.J. Babu, Amorphous-state characterization of efavirenz–polymer hot-melt extrusion systems for dissolution enhancement, J. Pharm. Sci. 101 (2012) 3456–3464.
[39] L.I. Mosquera-Giraldo, N.S. Trasi, L.S. Taylor, Impact of surfactants on the crystal growth of amorphous celecoxib, Int. J. Pharm. 461 (2014) 251–257.
[40] M. Mohsin, A. Hossin, Y. Haik, Thermomechanical properties of poly(vinyl alcohol) plasticized with varying ratios of sorbitol, Mat. Sci. Eng. A 528 (2011) 925–930.
[41] S. Tunç, O. Duman, The effect of different molecular weight of poly(ethylene glycol) on the electrokinetic and rheological properties of Na-bentonite suspensions, Colloids Surf. A Physicochem. Eng. Asp. 317 (2008) 93–99.
[42] L. Saravanan, S. Subramanian, Surface chemical studies on the competitive adsorption of poly(ethylene glycol) and ammonium poly(methacrylate) onto zirconia, Colloids Surf. A Physicochem. Eng. Asp. 252 (2005) 175–185.
[43] A.M.A. Elhissi, W. Ahmed, D. McCarthy, K.M.G. Taylor, A study of size, microscopic

morphology, and dispersion mechanism of structures generated on hydration of proliposomes, J. Dispers. Sci. Technol. 33 (2012) 1121–1126.
[44] M. Danaei, M. Dehghankhold, S. Ataei, F. Hasanzadeh Davarani, R. Javanmard, A. Dokhani, S. Khorasani, M.R. Mozafari, Impact of particle size and polydispersity index on the clinical applications of lipidic nanocarrier systems, Pharmaceutics 10 (2018) 57.
[45] C. Freitas, R.H. Müller, Effect of light and temperature on zeta potential and physical stability in solid lipid nanoparticle (SLN™) dispersions, Int. J. Pharm. 168 (1998) 221–229.
[46] S.G. Ong, L.C. Ming, K.S. Lee, K.H. Yuen, Influence of the encapsulation efficiency and size of liposome on the oral bioavailability of griseofulvin-loaded liposomes, Pharmaceutics 8 (2016) 25.
[47] N. Zhao, L.L. Augsburger, The influence of swelling capacity of superdisintegrants in different pH media on the dissolution of hydrochlorothiazide from directly compressed tablets, AAPS PharmSciTech 6 (2005) E120–E126.
[48] L.H. Nielsen, T. Rades, A. Mullertz, Stabilisation of amorphous furosemide increases the oral drug bioavailability in rats, Int. J. Pharm. 490 (2015) 334–340.
[49] M. Nasr, In vitro and in vivo evaluation of proniosomes containing celecoxib for oral administration, AAPS PharmSciTech 11 (2010) 85–89.
[50] S. Bozdag-Pehlivan, B. Subasi, I. Vural, N. Unlu, Y. Capan, Evaluation of drug-excipient interaction in the formulation of celecoxib tablets, Acta Pol. Pharm. 68 (2011) 423–433.
[51] R. Qi, Y.-Z. Li, C. Chen, Y.-N. Cao, M.-M. Yu, L. Xu, B. He, X. Jie, W.-W. Shen, Y.-N. Wang, M.A. van Dongen, G.-Q. Liu, M.M. Banaszak Holl, Q. Zhang, X. Ke, G5-PEG PAMAM dendrimer incorporating nanostructured lipid carriers enhance oral bioavailability and plasma lipid-lowering effect of probucol, J. Control. Release 210 (2015) 160–168.
[52] S.M. Fischer, J. Parmentier, S.T. Buckley, I. Reimold, M. Brandl, G. Fricker, Oral bioavailability of ketoprofen in suspension and solution formulations in rats: the influence of poloxamer 188, J. Pharm. Pharmacol. 64 (2012) 1631–1637.
[53] A. Hildebrand, K. Beyer, R. Neubert, P. Garidel, A. Blume, Temperature dependence of the interaction of cholate and deoxycholate with fluid model membranes and their solubilization into mixed micelles, Colloids Surf. B Biointerfaces 32 (2003) 335–351.
[54] M. Kuentz, Lipid-based formulations for oral delivery of lipophilic drugs, Drug Discov. Today Technol. 9 (2012) e97–e104.
[55] W.P. Battisti, N.P. Katz, A.L. Weaver, A.K. Matsumoto, A.J. Kivitz, A.B. Polis, G.P. Geba, Pain management in osteoarthritis: a focus on onset of efficacy–a comparison of rofecoxib, celecoxib, acetaminophen, and nabumetone across four clinical trials, J. Pain 5 (2004) 511–520.
[56] A. Menozzi, C. Pozzoli, E. Giovannini, E. Solenghi, D. Grandi, S. Bonardi, S. Bertini, V. Vasina, G. Coruzzi, Intestinal effects of nonselective and selective cyclooxygenase inhibitors in the rat, Eur. J. Pharmacol. 552 (2006) 143–150.
[57] L.M. Lichtenberger, J.J. Romero, E.J. Dial, Gastrointestinal safety and therapeutic efficacy of parenterally administered phosphatidylcholine-associated indomethacin in rodent model systems, Br. J. Pharmacol. 157 (2009) 252–257.
[58] R. Staples, A. Misher, J. Wardell, Gastrointestinal irritant effect of glycerin as compared with sorbitol and propylene glycol in rats and dogs, J. Pharm. Sci. 56 (1967) 398–400.
[59] S.D. Singh-Joy, V.C. McLain, Safety assessment of poloxamers 101, 105, 108, 122, 123, 124, 181, 182, 183, 184, 185, 188, 212, 215, 217, 231, 234, 235, 237, 238, 282, 284, 288, 331, 333, 334, 335, 338, 401, 402, 403, and 407, poloxamer 105 benzoate, and poloxamer 182 dibenzoate as used in cosmetics, Int. J. Toxicol. 27 (2008) 93–128.